EUKARYOTIC CELL, Mar. 2011, p. 435–444 Vol. 10, No. 3
1535-9778/11/$12.00 doi:10.1128/EC.00145-10

Fig1 Facilitates Calcium Influx and Localizes to Membranes Destined To Undergo Fusion during Mating in *Candida albicans*▽†

Meng Yang,[1]# Alexandra Brand,[1] Thyagarajan Srikantha,[2] Karla J. Daniels,[2] David R. Soll,[2] and Neil A. R. Gow[1]*

Aberdeen Fungal Group, School of Life Sciences & Medicine, Institute of Medical Science, University of Aberdeen, Foresterhill, Aberdeen AB25 2ZD, United Kingdom,[1] and Department of Biology, University of Iowa, Iowa City, Iowa 52242[2]

Received 10 June 2010/Accepted 3 December 2010

Few mating-regulated genes have been characterized in *Candida albicans*. *C. albicans FIG1* (Ca*FIG1*) is a fungus-specific and mating-induced gene encoding a putative 4-transmembrane domain protein that shares sequence similarities with members of the claudin superfamily. In *Saccharomyces cerevisiae*, Fig1 is required for shmoo fusion and is upregulated in response to mating pheromones. Expression of Ca*FIG1* was also strongly activated in the presence of cells of the opposite mating type. CaFig1-green fluorescent protein (GFP) was visible only during the mating response, when it localized predominantly to the plasma membrane and perinuclear zone in mating projections and daughter cells. At the plasma membrane, CaFig1-GFP was visualized as discontinuous zones, but the distribution of perinuclear CaFig1-GFP was homogeneous. Exposure to pheromone induced a 5-fold increase in Ca^{2+} uptake in mating-competent opaque cells. Uptake was reduced substantially in the *fig1*Δ null mutant. CaFig1 is therefore involved in Ca^{2+} influx and localizes to membranes that are destined to undergo fusion during mating.

Candida albicans is part of the normal microflora in the gastrointestinal tract and is also a clinically important opportunistic pathogen in humans. A parasexual mating pathway in this obligately diploid fungus has been investigated intensively over the last 10 years, and the studies have shown similarities to and distinct differences from the orthologous mating process in *Saccharomyces cerevisiae*. *C. albicans* mating may occur on or within the human body and has been shown to occur either through heterothallic or homothallic interactions (2, 16, 23, 28, 35, 36). Transcriptome studies showed that the mating response involved the upregulation of a specific set of genes via the transcription factor Cph1, which also regulates virulence factor expression and promotes filamentous growth. This suggests that the mating response in *C. albicans* may directly influence host-pathogen interactions as well as creating novel recombinant genotypes via genetic recombination (7, 55). Although the activity of pheromone-regulated transcription factors has been described, the function of their effectors has received less attention.

Unlike the case for mating in the haploid yeast *S. cerevisiae*, diploid *C. albicans* cells must first become homozygous at the mating-type locus (MTL), which promotes the switch from white yeast-shaped cells to mating-competent, bean-shaped opaque cells (22, 33, 36). The mechanism that leads to homozygosity *in vivo* is not well understood, but the genotype can be generated *in vitro* either by deletion of the *MTL***a** or *MTL*α genes or by plating cells on L-sorbose, which causes loss of one copy of chromosome 5 bearing the MTL (24, 35). *In vitro*, MTL-homozygous cells arise predominantly by the loss of one chromosome 5 homolog, followed by duplication of the retained homolog (51). MTL-homozygous cells switch to the opaque form at high frequency to produce mating-competent, pheromone-secreting mating partners that form shmoo mating projections (34). In the process of shmoo formation, pheromone-dependent chemotropism can occur in a biofilm which stabilizes chemotropic gradients, hence, facilitating the directed growth of mating projections toward each other (16). Chemotropism is followed by fusion and the formation of a tetraploid daughter cell (6).

In *S. cerevisiae*, calcium influx is essential for cell survival and efficient fusion of gametes during the mating process (17). In *C. albicans*, directional growth responses depend on the influx of calcium ions through calcium channels in the plasma membrane (10, 12). Two calcium uptake systems in *S. cerevisiae* have been described, and homologous systems in *C. albicans* have been identified (12, 37, 38). The high-affinity calcium uptake system (HACS), comprising the Mid1-Cch1 complex, is activated in low-Ca^{2+} medium and in response to alkaline, cold, iron, and endoplasmic reticulum (ER) stress (8, 40, 48). A third protein, Fig1 (mating factor-induced gene 1), was identified as a component of the low-affinity calcium uptake system (LACS) that was activated during growth in rich medium (37). In *C. albicans*, deletion of calcium channel gene *CCH1* or *MID1* reduced Ca^{2+} uptake during vegetative growth, but deletion of *FIG1* had no measurable effect on calcium ion transport in yeast or hyphal cells (12). However, Ca*fig1*Δ null mutants had altered hyphal tropic responses, suggesting that Ca*FIG1* was expressed at low levels during vegetative growth (12). *FIG1* expression was upregulated in both *S. cerevisiae* and *C. albicans* in response to mating pheromone (34, 38). In *S. cerevisiae*, *FIG1* expression increased 5- to 7-fold in response to

* Corresponding author. Mailing address: School of Life Sciences & Medicine, Institute of Medical Science, University of Aberdeen, Foresterhill, Aberdeen AB25 2ZD, United Kingdom. Phone: 44(0)1224-555879. Fax: 44(0)1224-555844. E-mail: n.gow@abdn.ac.uk.

Present address: Department of Molecular Microbiology, Washington University Medical School, St. Louis, MO.

▽ Published ahead of print on 7 January 2011.

† The authors have paid a fee to allow immediate free access to this article.

TABLE 1. Strains used in this study

Strain	Genotype	MTL	Reference(s)
CAI4	*ura3*Δ *iro1*Δ::*imm434*/*ura3*Δ *iro1*Δ::*imm434*	**a**/α	19, 20
NGY152	CAI4/CIp10, as CAI4, *RPS1*/*rps1*::pCIp10	**a**/α	11
NGY372	As CAI4, *fig1*Δ::*dpl200*/*fig1*Δ::*dpl200*/*RPS1*/*rps1*::pCIp10	**a**/α	12
NGY493	As CAI4, *FIG1*/*FIG1-GFP*	**a**/α	This study
NGY494	As CAI4, *FIG1*/*FIG1-GFP*	**a**/**a**	This study
NGY495	As CAI4, *FIG1*/*FIG1-GFP*	α/α	This study
NGY496	As CAI4, *RPS1*/*rps1*::placpoly6-P_{FIG1}	**a**/α	This study
NGY497	As CAI4, *RPS1*/*rps1*::placpoly6-P_{FIG1}	**a**/**a**	This study
NGY498	As CAI4, *RPS1*/*rps1*::placpoly6-P_{FIG1}	α/α	This study
NGY499	CAI4	−/α	This study
NGY500	CAI4	**a**/−	This study
NGY501	As CAI4, *fig1*Δ::*dpl200*/*fig1*Δ::*dpl200*/*RPS1*/*rps1*::pCIp10	−/α	This study
NGY502	As CAI4 *fig1*Δ::*dpl200*/*fig*Δ::*dpl200*/*RPS1*/*rps1*::pCIp10	**a**/−	This study
NGY576	As CAI4, *fig1*Δ::*dpl200*/*FIG1-GFP* (A)[a]	**a**/α	This study
NGY577	As CAI4, *fig1*Δ::*dpl200*/*FIG1-GFP* (B)[a]	**a**/α	This study

[a] Independent transformant.

mating pheromone and *S. cerevisiae* Fig1-green fluorescent protein (ScFig1-GFP) was distributed homogeneously in the plasma membrane of shmoos and to occasional reticular or punctate intracellular foci (38). Deletion of Sc*FIG1* resulted in incomplete fusion between the tips of mating shmoos, which was thought to be due to the loss of a calcium-dependent membrane repair mechanism (1, 38). Transcription profiling in *C. albicans* suggested that Fig1 function could be likewise predominantly associated with the mating process because white/opaque switching and exposure to mating pheromone caused a significant increase in *FIG1* gene expression (34).

There is no clear Fig1 homologue outside the fungal kingdom (17, 54), but the protein sequence contains characteristics found in the large mammalian PMP22/EMP/MP20/claudin superfamily (NCBI accession number pfam00822), the members of which selectively limit or promote paracellular ion flux across epithelial tight junctions and regulate the expression of proteins at the cell surface (44, 49). Sequence characteristics include four putative transmembrane domains and a conserved claudin motif [GΦΦGxC(n)C, where Φ is a hydrophobic amino acid and n is any number] in the large first extracellular loop (29, 45). Claudin-like proteins in fungi include Sur7 in *C. albicans* and Dni1 in *Schizosaccharomyces pombe*. Sur7 is an eisosome protein involved in plasma membrane organization and cell wall growth (4). In *S. pombe*, Dni1-GFP localized to sites of apposition between mating cells, and its deletion caused fusion defects which appeared to be due to membrane mislocalization (15). These two claudin-like proteins in fungi therefore appear to be involved in membrane dynamics.

In *C. albicans*, Fig1 has been associated with tip reorientation in response to environmental cues. Chemotropism of mating projections in response to pheromone and thigmotropism of vegetative hyphae require directionally regulated polarized growth (12, 17). The molecular processes involved in tip guidance are not well understood but appear to involve Ca^{2+} uptake (9). Both polarized growth morphologies are Cph1 dependent, and gene deletion and transcription studies indicate that Fig1 activity could be involved in Ca^{2+} influx and in tropic tip guidance (12, 14, 34). However, the role of Fig1 in shmoo orientation and in mating for *C. albicans* has not been defined. Therefore, in this study, we investigated the role of Fig1 during mating by studying calcium uptake, gene expression, and protein localization during the *C. albicans* mating process.

MATERIALS AND METHODS

Strains, culture conditions, and general genetic manipulation. The *C. albicans* strains used in this study are listed in Table 1. White and opaque cells were maintained on YPD agar (2% [wt/vol] peptone, 2% [wt/vol] glucose, 1% [wt/vol] yeast extract, 2% [wt/vol] agar) (Oxoid) at 30°C and 25°C, respectively. SD medium (0.67% [wt/vol] yeast nitrogen base [YNB] without amino acids [BD], 2% [wt/vol] glucose, 0.067% [wt/vol] complete supplement mix minus uracil [CMS-uracil; Qbiogene, Cambridge, United Kingdom]) or SD medium supplemented with 1 mg/ml 5-fluoroorotic acid (Melford) and 25 μg/ml uridine (Sigma) was used for selecting uridine prototrophs or auxotrophs, respectively. Strains with homozygosity (**a**/**a** or α/α) or hemizygosity (**a**/− or α/−) at the *MTL* locus were derived by L-sorbose selection (24) or by deletion mutagenesis (52), respectively. For monosomic chromosome 5 selection, colonies were grown on SD medium supplemented with 2% (wt/vol) L-sorbose instead of glucose. The presence of *MTL***a** and/or *MTL*α was verified by colony PCR using primers mtla5, mtla3, mtlα5, and mtlα3, listed in Table 2 (35). Deletion of the whole MTL was based on previously used methods using the nourseothricin resistance gene, Ca*SAT1*, as a selectable marker (52). Opaque cells were obtained from red sectors picked from colonies grown on YPD plates supplemented with 5 μg/ml phloxine B (cyanosine; Sigma) (5). Extensor PCR with proofreading activity (Thermo Scientific) was used for amplification of cassettes used for transformation.

Construction of FIG1-LacZ reporter. The genomic region between the stop codon of *orf19.137*, upstream of *FIG1*, and the *FIG1* start codon (315 bp) was amplified using primers FIG1plac-F and FIG1plac-R, containing restriction sites PstI and XhoI, respectively. The amplicon was poly(A)-tailed, purified, and ligated into plasmid pGEM-T Easy to generate plasmid pGEMT-P_{FIG1}. The pGEMT-P_{FIG1} fragment containing the *FIG1* promoter was excised by digestion with PstI and XhoI and ligated upstream of the promoterless *Streptococcus thermophilus lacZ* gene in plasmid placpoly6 (39) to generate plasmid placpoly6-P_{FIG1}. Correct ligation and orientation of the *FIG1* promoter was confirmed by PCR using primers FIG1plac-F and Clp10-GS. The placpoly6-P_{FIG1} plasmid possesses the *URA3* gene for selection in *C. albicans*. StuI-digested placpoly6-P_{FIG1} was targeted to the *RPS1* site in CAI4 (19). Transformants were analyzed by PCR using primers FIG1plac-F and Clp10-GS to verify genomic localization and Southern analysis to screen out transformants with multiple insertions.

Construction of *FIG1-GFP* fusions. Construction of the Fig1-GFP fusion protein was carried out using a PCR-based method described previously (19). In the CAI4 (*FIG1*/*FIG1*) or *fig1*Δ/*FIG1* (heterozygous) background, the stop codon of one of the *FIG1* alleles was replaced by the cassette containing *GFP* and the prototrophic marker *URA3* amplified from plasmid pGFP-URA3 by using long primers FIG1-GFP-F and FIG1-GFP-R. The fusion construct of *FIG1-GFP* was confirmed by PCR using primers CAI4-FIG1-F and xFG-f/F-R and by Southern blotting. Transcription of *GFP* was verified by reverse transcription-PCR (RT-PCR) using primers Meg17-F and Meg16-2-R (30).

TABLE 2. Oligonucleotide primers used in this study

Primer (reference)	Sequence (5′–3′)[a]
FIG1-GFP-F	TTTAAGTGCTTGTTTATCATGGTGGATGGAAATTAGAATGAGTAAATTGAATGGAAAATCACTGCAACACCAACAACAACCACTGGTGGATACAAAAATTGGTGGTGGTTCTAAAGGTGAAGAATTATT
FIG1-GFP-R	CTACATTGTTTATGAGTTGTTGATTTATTGACTTGTGTTGTTATGTCAGTAGAAGACTATAAACGGTTTTTATTGTATTTTTTTGGCAGAAATTTGTACATCTAGAAGGACCACCTTTGATTG
CAI4-FIG1-F	ATTATCCTTTGTTATTGTGTC
xFG-f/F-R	AAATTCTAACAAGACCATGTG
Meg17-F (30)	GGTTGAATTAGATGGTGATG
Meg16-R (30)	CATACCATGGGTAATACCAG
FIG1-plac-F	CGCATCTGCAGACCATTTTTAGCTACCATTGC
FIG1-plac-R	GGCTAGCTCGAGATACAATGGTGAATTTCAATGG
mtla5 (35)	TTGAAGCGTGAGAGGCAGGAG
mtla3 (35)	GTTTGGGTTCCTTCTTTCTCATT
mtlα5 (35)	TTTCGAGTACATTCTGGTCGCG
mtlα3 (35)	TGTAAACATCCTCAATTGTACCC
Clp10-GS	GTACATTCCTACTCCTGTTCG

[a] Underlining indicates region of homology with genomic DNA flanking the 3′ end of the *FIG1* gene.

Thigmotropism assay. Thigmotropism assays were carried out as previously described to determine whether the GFP-Fig1 allele was functional (12). Briefly, yeast cells were adhered to poly-L-lysine-coated quartz slides featuring ridges of 0.79 μm ± 40 nm and a pitch of 25 μm (Kelvin Nanotechnology, Glasgow, United Kingdom). Slides were incubated in 20 ml prewarmed 20% (vol/vol) newborn calf serum–2% (wt/vol) glucose at 37°C for 6 h. The number of hyphae reorienting on contact with a ridge was expressed as the percentage of the total observed interactions. A minimum of 100 interactions was observed per strain in each experiment, and results were reported as means ± standard errors from a minimum of 3 independent experiments.

Synthesis of α-factor peptide. The α-pheromone 13-mer peptide GFRLTNF GYFEPG (7) was synthesized by Open Biosystems. Freeze-dried powder was dissolved in dimethyl sulfoxide (DMSO) (Sigma) to 100 mg/ml as master stock solution and further diluted 10-fold in sterile water to make working stock solutions.

LacZ reporter of *FIG1* promoter activity. Stationary-phase cells carrying the FIG1p-LacZ construct were cross-streaked on SD agar by using replica plating. Plates were incubated for 48 h at room temperature. Cells were lysed by flooding the plate with 15 ml chloroform and incubating at room temperature for 5 min. Excess chloroform was poured off, and the plate was air dried in a flow hood for 10 min. Low-melting-point 1% agarose in 0.1 M sodium phosphate buffer containing 250 μg/ml X-Gal (5-bromo-4-chloro-3-indolyl-β-D-galactopyranoside) was poured at an approximate temperature of 45°C. Plates were sealed and incubated at 30°C overnight. For quantitative measurement of enzyme activity, a single opaque colony was inoculated into 10 ml YPD and incubated at 23°C for 48 h to reach stationary phase. The white/opaque ratio of the culture was verified by light microscopy. Opaque cells were subcultured into 100 ml fresh YPD at an optical density at 600 nm (OD_{600}) of 0.5 and incubated at 23°C for 5 h prior to the addition of pheromone. For positive controls, opaque cell suspensions were mixed at a 1:1 ratio in YPD without pheromone. After a further 12 h of incubation at 23°C, the OD_{600} was recorded and 10-ml samples were centrifuged and pellets stored at −20°C. For analysis, cell pellets were resuspended in 1 ml z buffer (60 mM Na_2HPO_4, 40 mM NaH_2PO_4, 10 mM KCl, 1 mM $MgSO_4$, 50 mM β-mercaptoethanol) in Eppendorf tubes. Chloroform (50 μl), SDS (0.1%), and samples were shaken vigorously for 5 min to lyse cells. Samples were prewarmed at 37°C, and then 200 μl of 4 mg/ml prewarmed ONPG (*o*-nitrophenyl-β-D-galactopyranoside) was added. After 2 h, 0.8 ml of the reaction mixture was removed and mixed with 0.4 ml 1 M Na_2CO_3 to stop the reaction. The cell debris was pelleted by centrifugation. The supernatant was removed and the optical density was read at a wavelength of 420 nm. Calculations of β-galactosidase (βgal) activities were based on the method of Munro et al. (39).

Imaging of mating by fluorescence microscopy. Both **a** and α opaque cells were grown in modified Lee's medium (MLM) (5a) to stationary phase. Samples of 0.5 ml of each mating type were mixed at a 1:1 ratio in 50 μl phosphate-buffered saline (PBS) (Oxoid), dropped onto YPD agar, and incubated at 25°C for 48 h. A sample of the mating mixture was washed once with PBS, centrifuged, and resuspended in 100 μl PBS. Nuclei and cell wall chitin were visualized using DAPI (4′,6-diamidino-2-phenylindole) (Roche Diagnostics GmbH) at 200 μg/ml in DMSO and 100 μg/ml calcofluor white (CFW) (Sigma), respectively. The styryl dye FM4-64 (Invitrogen) was used at 1 μg/ml for vacuole staining (46). For DAPI and CFW staining, samples were first incubated in CFW and then DAPI at room temperature for 45 min each and finally washed once with PBS. For FM4-64 and CFW costaining, cells were resuspended in 100 μl modified Lee's medium before FM4-64 was added and incubated at room temperature with agitation for 45 min. Cells were then washed once with modified Lee's medium and stained with CFW as described above. For microscopy, 5 μl of cell suspension was spotted onto a glass slide and covered with a coverslip, and the edges were sealed with a 1:1:1 mix of molten petrolatum, paraffin, and lanolin. Images were captured using a Delta Vision RT Deconvolution imaging system and processed using the Imaris Softworx suite version 1.3 (46).

Calcium uptake measurements. Opaque cells were grown in 5 ml modified Lee's medium at 25°C for 48 h until they reached stationary phase. The white/opaque ratio was determined by light microscopy, and cultures of >99% opaque cells were used for further analysis. Cells were washed twice in sterile H_2O and resuspended in 5 ml modified Lee's medium at 3×10^7 cells/ml. Ca^{2+} uptake was determined in mating mixtures, in which **a** and α cells were used at a 1:1 ratio and a density of 3×10^7 cells/ml or in *MTL***a** cells after the addition of α-pheromone to a final concentration of 10 μg/ml. Trace $^{45}Ca^{2+}$ (PerkinElmer) was added to cultures at time zero. The OD_{600} of the cell culture and uptake of $^{45}Ca^{2+}$ were determined at 12 h for mating cells or 3 h for α-pheromone-induced cells. Culture samples were filtered through glass microfiber paper disks (25-mm diameter) (Whatman, Kent, United Kingdom) by using a Millipore filtration unit. Filters were washed with 25 ml buffer containing 5 mM Ca^{2+} and dried at 80°C for 45 min. $^{45}Ca^{2+}$ activity was measured by liquid scintillation counting.

Bioinformatic analysis. Candidate protein transmembrane topology was analyzed using Phobius. NetNGlyc was used for prediction of N-glycosylation sites. *FIG1* orthologues were aligned using ClustalW from the European Bioinformatics Institute (EBI).

RESULTS

Orthologous Fig1 structure and conserved motifs. Researchers have identified Fig1 orthologues in the sequenced genomes from the *Ascomycota* group but not in those from the basidiomycetes, *Ustilago maydis*, or zygomycete *Rhizopus oryzae* (42). Sequence alignment using ClustalW showed that all orthologues contained 4 potential transmembrane (TM) domains, with two conserved motifs in the predicted extracellular loop region between TM1 and TM2 (Fig. 1A and B). The glycine-cysteine motif was conserved in all species, with the exception of *Debaromyces hansenii*, and located at the C terminus of TM1. The second domain, GΦΦGxC(n)C, is a feature of the claudin superfamily. With the exception of the *Pezizomycotina* subgroup that consisted of 3 *Aspergillus* species, all species contained 1 to 4 potential N-glycosylation sites in the TM1-TM2 intervening region. Within the claudin super-

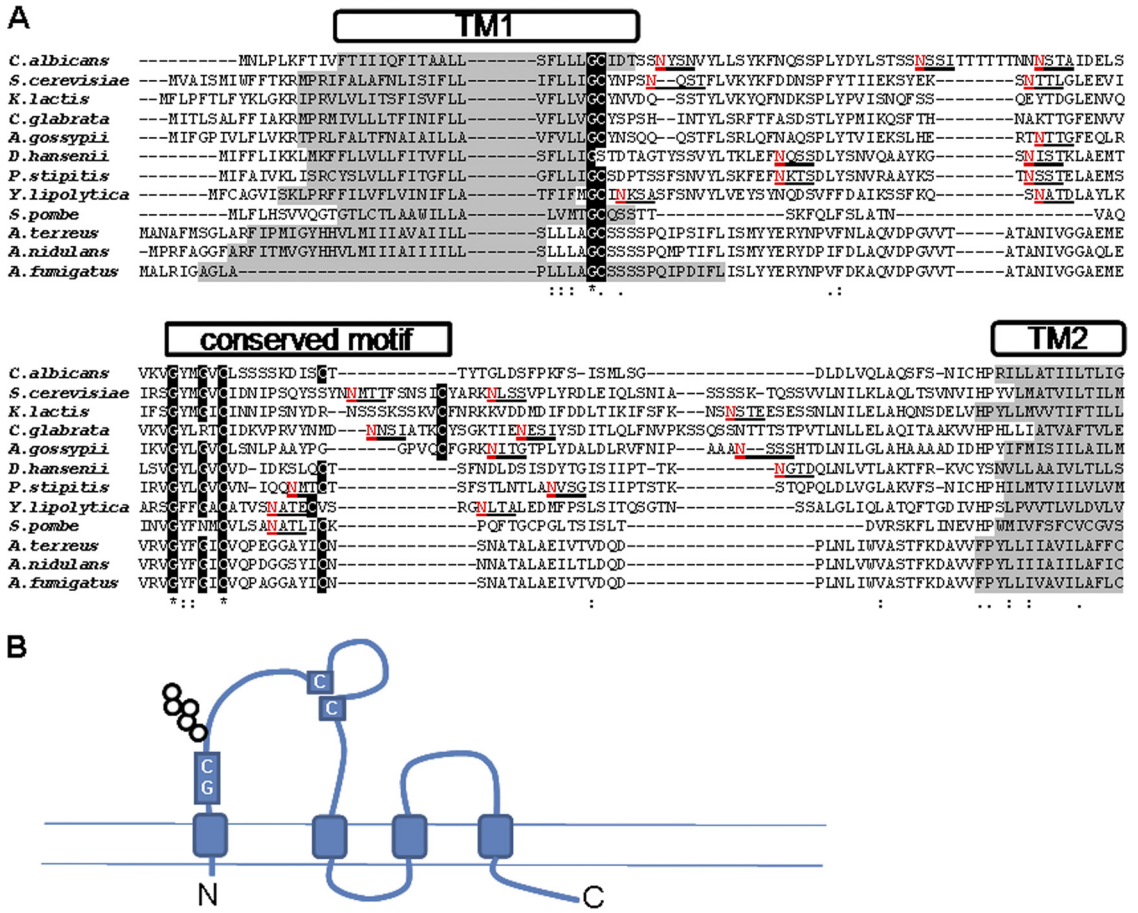

FIG. 1. Predicted structure and conserved motifs in fungal orthologues of Fig1. (A) The amino acid sequences of the extracellular regions of Fig1 orthologues from 12 sequenced *Ascomycota* fungal species were aligned using ClustalW. Areas with a gray background indicate putative hydrophobic transmembrane domains predicted using Phobius. Highly conserved amino acid residues are highlighted with a black background and constitute a conserved Gly-Cys motif and a second conserved motif that is characteristic of the claudin superfamily. Putative N-glycosylation sites, predicted by NetNGlyc, are underlined, and the modified asparagine residues are shown in red. *K. lactis*, *Kluyveromyces lactis*; *C. glabrata*, *Candida glabrata*; *A. gossypii*, *Ashbya gossypii*; *P. stipitis*, *Pichia stipitis*; *Y. lipolytica*, *Yarrowia lipolytica*; *A. terreus*, *Aspergillus terreus*; *A. nidulans*, *Aspergillus nidulans*; *A. fumigatus*, *Aspergillus fumigatus*. *, identical; :, conserved substitution; ·, semiconserved. (B) The predicted structure of the Fig1 protein family suggests that there are four transmembrane domains giving rise to two extracellular loops. The conserved Gly-Cys, N-glycosylation, and claudin motifs are contained within loop 1.

family, the positioning of N-glycosylation sites between TM1 and TM2 is a characteristic of the EMP (epithelial membrane protein) subgroup (44).

FIG1 deletion reduces calcium uptake under mating conditions. To determine whether Fig1 is involved in Ca^{2+} uptake during mating in *C. albicans*, mating-competent **a** or α (*MTL*-homozygous) *fig1*Δ deletion mutants were generated from a parent *MTL***a**/α strain, NGY372 (12). Homozygous *fig1*Δ **a** (NGY502) and *fig1*Δ α (NGY501) strains underwent normal white/opaque switching (data not shown). The accumulation of $^{45}Ca^{2+}$ in a 1:1 mixed population of opaque mating-competent control strains, CAI4 **a** (NGY500) and CAI4 α (NGY499), increased 5-fold over a 12-h period, indicating that Ca^{2+} uptake occurs during mating in *C. albicans* (Fig. 2A). A similar increase was observed when the CAI4 **a** strain was exposed to α-pheromone (Fig. 2B). Deletion of *FIG1* did not affect Ca^{2+} accumulation in unstimulated cells, but reduced levels of uptake occurred in *fig1* null mutants in mating populations and in *fig1 MTL***a** cells that were treated with α-pheromone.

FIG1* expression is activated by α-pheromone and mating.** Activation of the *FIG1* promoter was assayed using strains bearing the *FIG1* promoter inserted upstream of the *LACZ* reporter gene. Opaque-phase *MTLa** and *MTL*α control strains carrying the *FIG1*p-LacZ reporter construct (*FIG1*p-*LacZ* **a** and *FIG1*p-*LacZ* α strains) were cross-streaked on solid YPD agar and incubated at room temperature for 48 h. Whole-plate images were photographed following cell lysis and overlay of X-Gal. Blue pigment was visible only where streaks of cells of opposite mating types carrying the *FIG1*p-LacZ reporter intersected, indicating that *FIG1* expression was activated when mixed populations of *MTL***a** and *MTL*α occurred together but not in populations with homogeneous mating types (Fig. 3A). As predicted, fainter blue pigment was observed at the intersection of Fig1p-LacZ-carrying strains of either mating type with cells carrying no reporter. Shmoo formation and cell fusion were observed in all cell samples picked from the cross-streaked intersections and viewed by light microscopy (Fig. 3B), indicating that the *FIG1* promoter was activated in cells of both mating types.

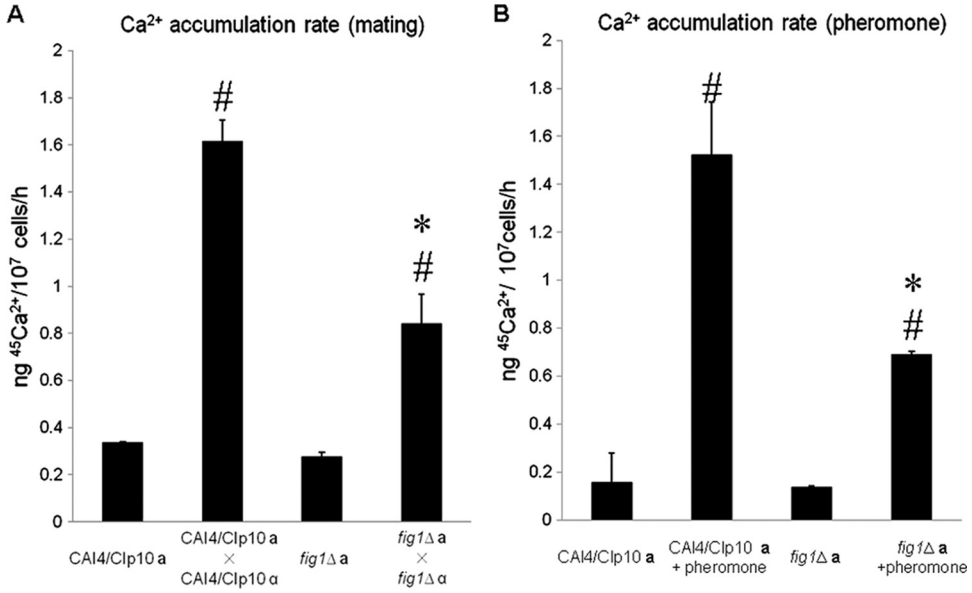

FIG. 2. The effect of *FIG1* deletion on calcium uptake under mating conditions. (A) Uptake of $^{45}Ca^{2+}$ in mating populations of the control strain or the *fig1*Δ mutant was determined by mixing mating-competent **a** and α opaque cells at a ratio of 1:1. (B) Uptake of $^{45}Ca^{2+}$ in cultures of mating-competent CAI4/CIp10 **a** (NGY500) cells or *fig1*Δ **a** (NGY502) cells, with and without the addition of 10 μg/ml α-pheromone, was determined. Means and standard deviations (error bars) were from two independent experiments. Asterisks denote a significant difference from the value obtained for the control strain under same treatment. Number signs indicate a significant difference from the value for the relevant untreated control strain ($P < 0.05$ [two-tailed Student's *t* test]).

Opaque-phase *MTL***a** and *MTL*α control strains carrying the *FIG1*p-LacZ reporter construct (*FIG1*p-*LacZ* **a** and *FIG1*p-*LacZ* α strains) were mixed in a 1:1 ratio in liquid MLM and incubated at 25°C for 12 h. Colorimetric analysis showed that exposure to cells of opposite mating types induced a 16-fold increase in *FIG1* expression compared to that of populations of a single mating type (Fig. 3C). Opaque, mating-competent *FIG1*p-*LacZ* **a** cells grown in liquid YPD medium were exposed to increasing concentrations of synthetic 13-mer α-pheromone for a period of 12 h. α-Pheromone at a concentration of 0.1 μg/ml failed to induce a detectable increase of *FIG1* promoter activity over that observed in unstimulated cells, but activity increased in a dose-dependent manner on exposure to 10-fold increases in the α-pheromone concentration (Fig. 3C). From this, the concentration of pheromone produced by the mixture of mating cells in 12-h cultures was estimated to be around 5 μg/ml.

Dynamics of Fig1-GFP expression. To visualize Fig1-GFP expression and localization in single cells during shmoo formation and mating, an enhanced GFP cassette containing the *URA3* auxotrophic marker was fused to the C terminus of the Fig1 protein in the *FIG1*/*FIG1* and *fig1*Δ/*FIG1* genetic backgrounds. *FIG1-GFP* was therefore under the transcriptional control of the native *FIG1* promoter (21). To test whether the Fig1-GFP fusion was functional, strains harboring a single GFP-tagged allele of *FIG1* were assayed for their ability to reorient their growing tips on contact with ridges in the substrate. In previous studies, the *fig1*Δ/*fig1*Δ null mutant was significantly defective in this thigmotropic response (12). The two *fig1*Δ/*FIG1-GFP* independent transformants (NGY576 and NGY577) exhibited thigmotropic responses that were not significantly different from those of the control strain, unlike the null mutant, which was defective in thigmotropism (Fig. 4A). This suggests that *FIG1-GFP* was functional. The same result was observed for the *FIG1*/*FIG1-GFP* (NGY493) strain. This strain was used to generate mating-competent *FIG1-GFP* **a** (NGY494) and *FIG1-GFP* α (NGY495) strains by selection on L-sorbose, followed by PCR screening for the two mating type alleles. Opaque cells were picked and restreaked from sectored white cell colonies grown in the presence of phloxine B. *FIG1-GFP* **a** cells were exposed to 50 μg/ml α-pheromone for a period of 12 h, and images were captured using time-lapse fluorescence microscopy. Fig1-GFP was detectable at the site of shmoo formation 40 to 60 min after the addition of α-pheromone, as the emerging shmoo tip itself became visible (Fig. 4B). Fig1-GFP localized primarily to the shmoo apices. Fig1-GFP associated with the entire shmoo structure during the early stages but became tip biased in more elongated cells after 4 h of pheromone exposure (Fig. 4C). The same Fig1-GFP distribution was observed in populations of mating cells on YPD agar (Fig. 5A).

Contrasting distribution patterns of Fig1-GFP in the shmoo plasma membrane and the nuclear periphery. Fig1-GFP was visualized by fluorescence microscopy in shmoos produced in populations of *MTL***a** and *MTL*α cells mixed at a ratio of 1:1 (Fig. 5A). By using deconvolution microscopy, we observed Fig1-GFP as discontinuous zones at the periphery of the shmoo and in continuous intracellular structures within the shmoo, the body of the mother cell, and the newly formed daughter cell (Fig. 5A). In order to identify the intracellular structures associated with Fig1-GFP, mating cells were stained with DAPI (for nuclei), FM4-64 (for vacuoles), and CFW (for walls). The discontinuous microdomains of Fig1-GFP were immediately adjacent to the CFW-stained cell wall, suggesting

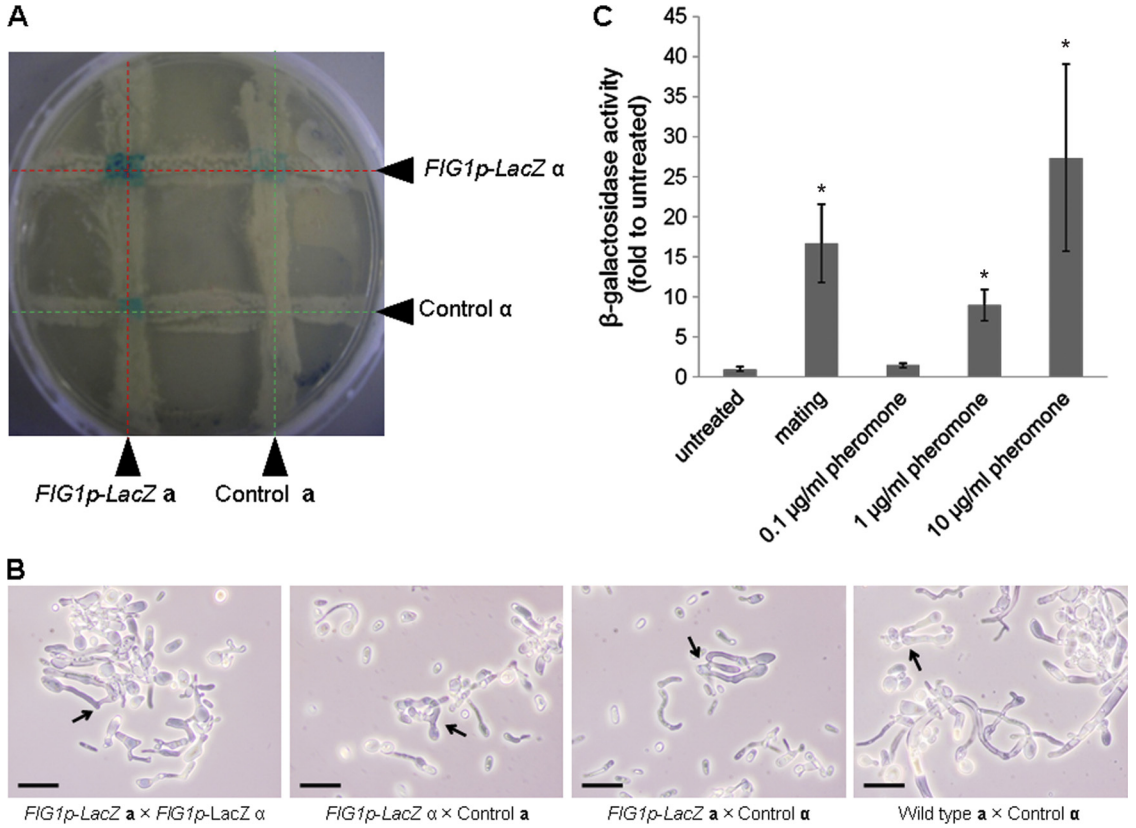

FIG. 3. Fig1 promoter activation in response to pheromone and cells of the opposite mating type. (A) *MTL*α and *MTL***a** cells of the control strain were cross-streaked on YPD agar with *MTL*α and *MTL***a** cells carrying the *FIG1*p-LacZ reporter. After 48 h of incubation at 25°C, β-galactosidase activity was determined by the appearance of blue pigment, indicating transcription of *LacZ* driven by the activated *FIG1* promoter. (B) The morphology of cells taken from the four cross-streaked intersections was viewed by light microscopy. Arrows indicate mating events. Scale bars = 10 μm. (C) *FIG1*p-*LacZ* **a** cells were mixed with *FIG1*p-*LacZ* α (NGY498) cells in YPD medium at a 1:1 ratio and incubated at 25°C. *FIG1*p-*LacZ* **a** (NGY497) cells were treated with α-pheromone at increasing concentrations (0.1, 1.0, and 10 μg/ml). Promoter activity was measured in triplicate in a colorimetric β-galactosidase activity assay in 3 independent experiments. Asterisks indicate significant differences ($P < 0.05$; two-tailed Student's *t* test) compared to the value for the untreated sample. Error bars represent standard deviations.

that Fig1-GFP localized to the plasma membrane (Fig. 5B). In contrast, the continuous zones of Fig1-GFP surrounded the nuclear regions, suggesting that it localized to the proximal ER or the nuclear periphery (Fig. 5C and 6). Perinuclear Fig1-GFP persisted during nuclear migration and fusion and was still present at the nuclear periphery in the newly formed daughter cell (Fig. 5A, panels 4 and 5). Elongated DAPI-stained structures that were not associated with Fig1-GFP were observed in the shmoo, possibly representing the localization of mitochondrial DNA (Fig. 6C and F). Fig1-GFP was not detectable in the FM4-64-stained endosomal and vacuolar membranes (Fig. 6). This suggests that Fig1-GFP was not targeted to the vacuole for degradation at a significant rate in shmooing cells.

DISCUSSION

Fig1 as a member of the claudin superfamily. Fig1 is a member of a fungus-specific family of proteins that contains sequence characteristics found in the large mammalian PMP22/EMP/MP20/claudin (pfam00822). Claudins combine as dynamic multimeric complexes at the cell membrane. It is thought that their basic function lies in cell-cell adhesion. Claudins are also found in the epithelia of invertebrates, which lack tight junctions, where they are thought to perform a signaling function (50). The family includes regulators of solute movement through epithelial tight junctions, scaffolding proteins for the assembly of adhesion and receptor complexes, and γ subunits for the membrane delivery of the large α subunit of voltage-dependent calcium channels (reviewed by Van Itallie and Anderson [45]). In mammalian epithelia, claudins form ion-selective intercellular pores, but there is no evidence that they directly admit ions across the plasma membrane into the cell. Although Fig1 is involved in Ca^{2+} uptake, its lack of homology to any known ion influx channel suggests that its role may be as an indirect facilitator of Ca^{2+} influx.

We generated a series of mutant strains that were of the *MTL***a** or *MTL*α mating type in order to study Fig1 activity under conditions in which the gene was predicted to be highly expressed. Specifically, the aim was to determine whether *FIG1* is involved in Ca^{2+} uptake in *C. albicans* and to understand more about its role during polarized growth and mating.

Fig1-GFP localizes to shmoo apices during mating. In a time course study, expression of Fig1-GFP, controlled by the native Ca*FIG1* promoter, was easily detectable by fluorescence mi-

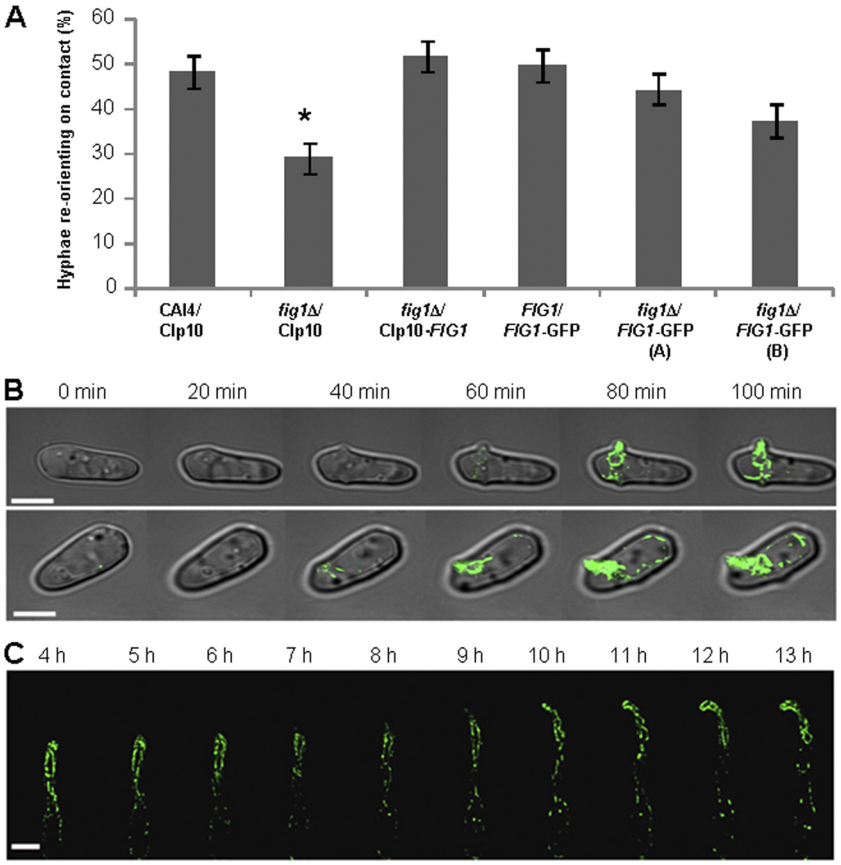

FIG. 4. Temporal expression and localization of Fig1-GFP during shmoo formation and extension. (A) Cells expressing a single copy of *FIG1-GFP* show normal contact-sensing responses to a ridged substrate (error bars represent standard errors of the means [$n = 3$]). Asterisk indicates a significant difference compared to the control strain ($P < 0.01$; Dunnett's t test). (B) Bean-shaped mating-competent *FIG1-GFP* **a** cells in modified Lee's medium were treated with 50 μg/ml α-pheromone, and image capture commenced immediately for a period of 100 min. (C) Cells were treated at 0 h (time zero) with 50 μg/ml α-pheromone. Image capture started at 4 h and continued until 13 h. Scale bars = 5 μm.

croscopy on exposure of **a** cells to α-pheromone. Fig1-GFP was observed at the site of mating projection formation, approximately 50 min after exposure to mating pheromone. Fig1-GFP was visible at the cell periphery and in reticular structures throughout the cell but localized predominantly within the mating projection. The reticular distribution in *C. albicans* contrasted with the pattern observed using a ScFig1::βgal fusion protein during shmoo formation in *S. cerevisiae*, where Fig1 appeared as punctate spots at the cell periphery (17). By use of deconvolution microscopy of *C. albicans* cells, we found the distribution of Fig1-GFP at the cell membrane to be discontinuous, which suggested that it may be present in microdomains. CFW staining showed that Fig1-GFP appeared in flattened zones in apposition with the cell wall. The intracellular reticular structures carrying Fig1-GFP localized within bright, perinuclear regions that persisted throughout shmoo formation and cell-cell fusion and in nuclei of the newly formed daughter cell. It is possible that the perinuclear localization of Fig1-GFP resulted from its biosynthesis in the ER. However, many other mating-induced genes, such as *FUS1* and *PRM1*, whose expression is induced in other fungi during mating, do not accumulate in the ER or the nuclear periphery (18, 41). Furthermore, Fig1-GFP was not visualized in the FM4-64-stained vacuolar membrane during shmoo elongation. Low levels of expression of ScFig1::βgal were visible in the perinuclear zone in *S. cerevisiae* cells prior to treatment with mating pheromone, supporting the possibility that Fig1 may have a second nuclear function (17). It has been reported that in mammalian cells, perinuclear Ca^{2+} release affects nuclear Ca^{2+} much more strongly than distal Ca^{2+} influx and a sustained rise in nuclear [Ca^{2+}] is required for calcineurin-NFAT (the Ca*CRZ1* product homologue) and cyclic AMP response binding element (CREB) signaling (13, 27, 31, 43). Fig1 may also have a general role in limiting membrane damage or promoting membrane fusion of the nuclear envelope and at the plasma membrane, both of which undergo fusion during mating.

Mating-dependent Fig1 expression and Ca^{2+} uptake in *C. albicans*. Ca^{2+} uptake increased approximately 5-fold in mixtures of opaque *MTL***a** or *MTL*α cells, and in *MTL***a** cells treated with α-pheromone (10 μg/ml), an 8- to 10-fold increase in Ca^{2+} uptake compared to that of untreated controls was observed. Together, these results demonstrate that exposure to mating pheromone in *C. albicans* mating-competent cells causes a significant increase in the intracellular [Ca^{2+}], as seen in *S. cerevisiae* (38). Deletion of *FIG1* in *C. albicans* reduced Ca^{2+} uptake to 50% of the control level, confirming that Fig1 is involved in Ca^{2+} influx but implying that mating also in-

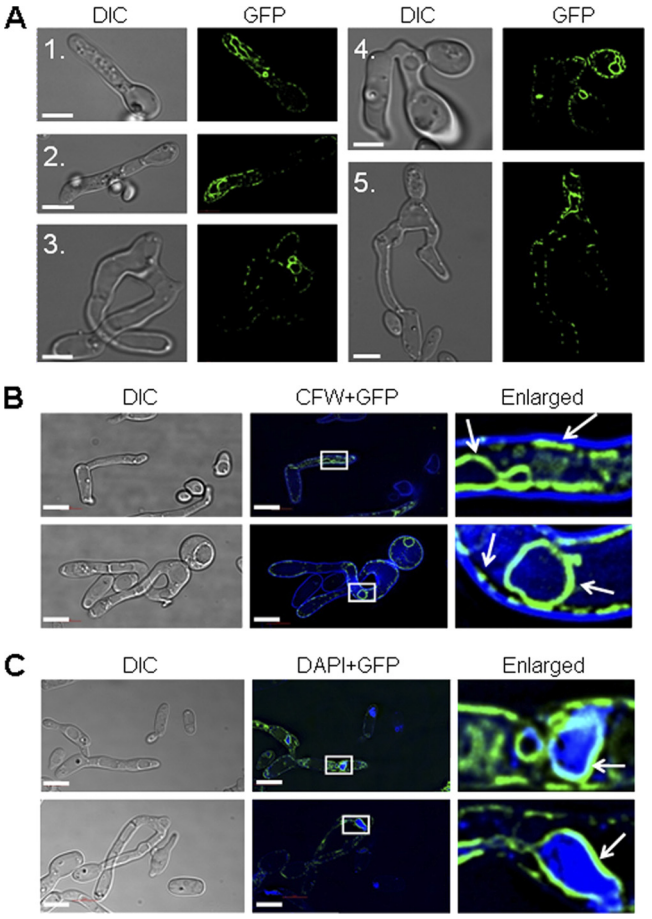

FIG. 5. Fig1-GFP localization in shmoos and fused cells. (A) *FIG1-GFP* **a** (NGY494) and *FIG1-GFP* α (NGY495) cells were mixed at a ratio of 1:1, spotted on 2% YPD agar, and incubated for 48 h at 25°C. Cells were taken from the plate and viewed by fluorescence microscopy. Fig1-GFP was observed in shmoos (panels 1 and 2), a zygote (panel 3), and daughter cells (panels 4 and 5). Cell wall chitin was stained with 100 μg/ml CFW. Fig1-GFP (green) localized in microdomains adjacent to the CFW-chitin wall layer (blue; arrows) (B) and more homogeneously adjacent to DAPI-stained perinuclear regions (enlarged image) (C). DIC, differential interference contrast. Scale bars = 5 μm.

volves Fig1-independent Ca^{2+} uptake. The Fig1-LacZ reporter construct was activated in both MTL mating types, demonstrating that this pathway forms part of a general mating response and is not MTL specific. In addition, the level of activity of the Fig-LacZ reporter construct increased in a pheromone dose-dependent manner. Taken together, these results suggest a positive correlation between pheromone concentration, Fig1 expression, and Ca^{2+} uptake. Mid1-Cch1, the HACS complex, may therefore also contribute to Ca^{2+} uptake during mating in *C. albicans*. HACS expression is influenced by the calcineurin-*CRZ1* Ca^{2+}-dependent signaling pathway in *C. albicans*, but its expression is not thought to be highly regulated (26). We have not been able to visualize Cch1-GFP or Mid1-GFP in *C. albicans*, but in *S. cerevisiae*, Mid1-GFP was visualized at the plasma membrane and in an ER-like zone around the nucleus in nonmating conditions and did not relocalize to the shmoo on treatment with mating pheromone (25, 32, 53). The highly enriched and spatially distinct domains of Fig1-GFP at the shmoo plasma membrane suggest that the functions of the two Ca^{2+} uptake systems differ during mating and that Fig1 might be involved in the generation of Ca^{2+} signals at specific sites. It has been reported that both chelation of extracellular Ca^{2+} and deletion of *FIG1* dramatically reduced mating efficiency of *C. albicans* (3). Our finding that Fig1 is involved in 50% of the Ca^{2+} uptake during mating confirms its importance in the mating process.

Mating-independent Fig1 expression. We previously identified Fig1 as a protein required for the normal thigmotropic response by *C. albicans*, where *FIG1* deletion significantly reduced the ability of hyphal tips to reorient on contact with ridges in the underlying substrate; this role of Fig1 is in contrast to its mating-dependent functions (12). All hyphal tropisms we have studied to date have been shown to be dependent on Ca^{2+} influx, but deletion of *FIG1* did not affect Ca^{2+} uptake during vegetative growth. Although *FIG1* mRNA was detected under all growth conditions tested, including in kidney tissue isolated from infected mice, a Fig1-GFP construct in yeasts or hyphae could not be visualized. This suggests that Fig1 is present at very low levels during vegetative growth but

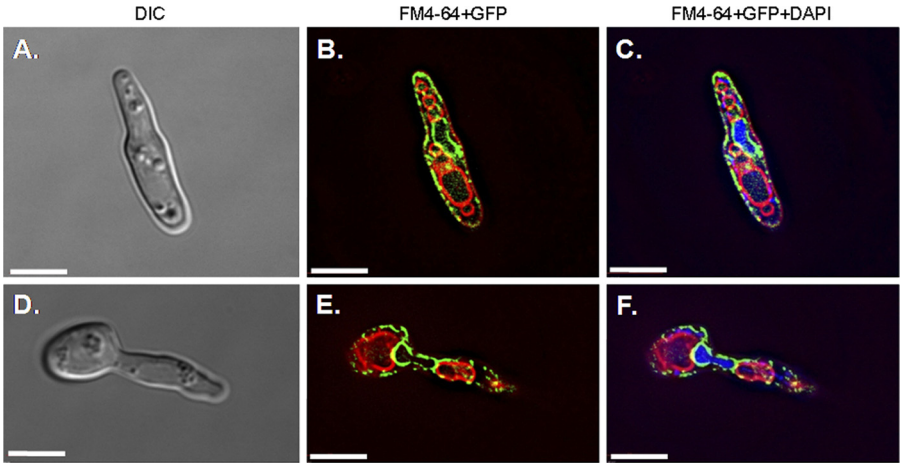

FIG. 6. Fig1 in shmooing cells from mating mixtures of *FIG1-GFP* **a** and *FIG1-GFP* α cells stained with DAPI (200 μg/ml) and FM4-64 (1 μg/ml). Scale bars = 5 μm.

that even basal level expression of Fig1 influences hyphal growth and orientation.

It is possible that the function and activity of Fig1 depend on its colocalization with other effectors. Two lines of evidence in *S. cerevisiae* suggest that ScFig1 has Ca^{2+}-related and Ca^{2+}-unrelated functions. First, output from the aequorin/Ca^{2+} reporter peaked during mating, while Fig1-Myc levels remained high, which suggested that Fig1 was still required in the plasma membrane after mating-induced Ca^{2+} uptake was complete (38). Second, mating-induced rapid cell death was found to be dependent on Fig1 but independent of its Ca^{2+} uptake activity (54). The involvement of other effectors in Fig1 function is suggested by the observation that membrane localization of Fig1 was necessary but not sufficient for LACS activity (38). In *C. albicans*, Fig1-GFP localization appeared to be perinuclear and at the plasma membrane. Both membranes are sites of membrane perturbation and fusion during mating. Fig1 was proposed to be necessary in *S. cerevisiae* for limiting the zone of membrane fusion during mating (38). *FIG1* deletion in *S. cerevisiae* resulted in defective cell fusion during mating, with undissolved wall material at the fusion site, which was rescued by the addition of extracellular Ca^{2+}. Such fusion defects were not observed in *fig1* null mutants of *C. albicans*, but Fig1 could nevertheless function to stabilize membranes in response to perturbation during polarized growth, possibly by limiting membrane expansion during critical stages in morphological change. Two observations provide evidence for this. First, *FIG1* deletion resulted in hypha formation on solid SD medium, while the control strain grew as yeast (12). This suggests that Fig1 may be a negative regulator of polarized growth in certain conditions. Second, *FIG1* deletion decreases the likelihood that hyphae will reorient the growth axis on contact with a small obstacle (12). Thus, although Fig1 is undoubtedly upregulated as part of the mating signaling pathway, its role may well be more generally related to membrane stability during morphological transitions, whether internally or externally induced. Fig1 therefore participates in the polarized growth of both mating projections and vegetative fungal hyphae, presumably by regulating calcium ion uptake at sites of polarized tip growth. *FIG1* expression represents a convenient marker for the mating process, but low levels of Fig1 in nonmating cells also influence the physiology of growth and development of *C. albicans*.

ACKNOWLEDGMENTS

This work was supported by the Signalpath EC Marie Curie Actions funding network (a studentship for M.Y. and BBSRC grant BB/E008372/1 to A.B.), and it was funded in part by the Developmental Studies Hybridoma Bank at Iowa, an NIH National Resource. We also acknowledge funding from the BBSRC (SABR) and the Wellcome Trust.

REFERENCES

1. **Aguilar, P. S., A. Engel, and P. Walter.** 2007. The plasma membrane proteins Prm1 and Fig1 ascertain fidelity of membrane fusion during yeast mating. Mol. Biol. Cell **18:**547–556.
2. **Alby, K., D. Schaefer, and R. J. Bennett.** 2009. Homothallic and heterothallic mating in the opportunistic pathogen *Candida albicans*. Nature **460:**890–893.
3. **Alby, K., D. Schaefer, R. K. Sherwood, S. K. Jones, Jr., and R. J. Bennett.** 2010. Identification of a cell death pathway in *Candida albicans* during the response to pheromone. Eukaryot. Cell **9:**1690–1701.
4. **Alvarez, F. J., L. M. Douglas, A. Rosebrock, and J. B. Konopka.** 2008. The Sur7 protein regulates plasma membrane organization and prevents intracellular cell wall growth in *Candida albicans*. Mol. Biol. Cell **19:**5214–5225.
5. **Anderson, J. M., and D. R. Soll.** 1987. Unique phenotype of opaque cells in the white-opaque transition of *Candida albicans*. J. Bacteriol. **169:**5579–5588.

5a. **Bedell, G. W., and D. R. Soll.** 1979. Effects of low concentrations of zinc on the growth and dimorphism of *Candida albicans*: evidence for zinc-resistant and -sensitive pathways for mycelium formation. Infect. Immun. **26:**348–354.

6. **Bennett, R. J., M. G. Miller, P. R. Chua, M. E. Maxon, and A. D. Johnson.** 2005. Nuclear fusion occurs during mating in *Candida albicans* and is dependent on the *KAR3* gene. Mol. Microbiol. **55:**1046–1059.
7. **Bennett, R. J., M. A. Uhl, M. G. Miller, and A. D. Johnson.** 2003. Identification and characterization of a *Candida albicans* mating pheromone. Mol. Cell. Biol. **23:**8189–8201.
8. **Bonilla, M., and K. W. Cunningham.** 2003. Mitogen-activated protein kinase stimulation of Ca^{2+} signaling is required for survival of endoplasmic reticulum stress in yeast. Mol. Biol. Cell **14:**4296–4305.
9. **Brand, A., and N. A. Gow.** 2009. Mechanisms of hypha orientation of fungi. Curr. Opin. Microbiol. **12:**350–357.
10. **Brand, A., K. Lee, B. Veses, and N. A. Gow.** 2009. Calcium homeostasis is required for contact-dependent helical and sinusoidal tip growth in *Candida albicans* hyphae. Mol. Microbiol. **71:**1155–1164.
11. **Brand, A., D. M. MacCallum, A. J. P. Brown, N. A. R. Gow, and F. C. Odds.** 2004. Ectopic expression of *URA3* can influence the virulence phenotypes and proteome of *Candida albicans* but can be overcome by targeted reintegration of *URA3* at the *RPS10* locus. Eukaryot. Cell **3:**900–909.
12. **Brand, A., et al.** 2007. Hyphal orientation of *Candida albicans* is regulated by a calcium-dependent mechanism. Curr. Biol. **17:**347–352.
13. **Chawla, S., G. E. Hardingham, D. R. Quinn, and H. Bading.** 1998. CBP: a signal-regulated transcriptional coactivator controlled by nuclear calcium and CaM kinase IV. Science **281:**1505–1509.
14. **Chen, J., J. Chen, S. Lane, and H. Liu.** 2002. A conserved mitogen-activated protein kinase pathway is required for mating in *Candida albicans*. Mol. Microbiol. **46:**1335–1344.
15. **Clemente-Ramos, J. A., et al.** 2009. The tetraspan protein Dni1p is required for correct membrane organization and cell wall remodelling during mating in *Schizosaccharomyces pombe*. Mol. Microbiol. **73:**695–709.
16. **Daniels, K. J., T. Srikantha, S. R. Lockhart, C. Pujol, and D. R. Soll.** 2006. Opaque cells signal white cells to form biofilms in *Candida albicans*. EMBO J. **25:**2240–2252.
17. **Erdman, S. E., L. Lin, M. Malczynski, and M. Snyder.** 1998. Pheromone-regulated genes required for yeast mating differentiation. J. Cell Biol. **140:**461–483.
18. **Fleissner, A., S. Diamond, and N. L. Glass.** 2009. The *Saccharomyces cerevisiae PRM1* homolog in *Neurospora crassa* is involved in vegetative and sexual cell fusion events but also has postfertilization functions. Genetics **181:**497–510.
19. **Fonzi, W. A., and M. Y. Irwin.** 1993. Isogenic strain construction and gene mapping in *Candida albicans*. Genetics **134:**717–728.
20. **García, M. G., J.-E. O'Connor, L. L. Garcia, S. I. Martinez, E. Herrero, and L. del Castillo Agudo.** 2001. Isolation of a *Candida albicans* gene, tightly linked to *URA3*, coding for a putative transcription factor that suppresses a *Saccharomyces cerevisiae aft1* mutation. Yeast **18:**301–311.
21. **Gerami-Nejad, M., J. Berman, and C. Gale.** 2001. Cassettes for the PCR-mediated construction of green, yellow, and cyan fluorescent protein fusions in *Candida albicans*. Yeast **18:**859–864.
22. **Hull, C. M., and A. D. Johnson.** 1999. Identification of a mating type-like locus in the asexual pathogenic yeast *Candida albicans*. Science **285:**1271–1275.
23. **Hull, C. M., R. M. Raisner, and A. D. Johnson.** 2000. Evidence for mating of the "asexual" yeast *Candida albicans* in a mammalian host. Science **289:**307–310.
24. **Janbon, G., F. Sherman, and E. Rustchenko.** 1999. Appearance and properties of L-sorbose-utilizing mutants of *Candida albicans* obtained on a selective plate. Genetics **153:**653–664.
25. **Kanzaki, M., et al.** 1999. Molecular identification of a eukaryotic, stretch-activated nonselective cation channel. Science **285:**882–886.
26. **Karababa, M., et al.** 2006. *CRZ1*, a target of the calcineurin pathway in *Candida albicans*. Mol. Microbiol. **59:**1429–1451.
27. **Kornhauser, J. M., et al.** 2002. CREB transcriptional activity in neurons is regulated by multiple, calcium-specific phosphorylation events. Neuron **34:**221–233.
28. **Lachke, S. A., S. R. Lockhart, K. J. Daniels, and D. R. Soll.** 2003. Skin facilitates *Candida albicans* mating. Infect. Immun. **71:**4970–4976.
29. **Lal-Nag, M., and P. Morin.** 2009. The claudins. Genome Biol. **10:**235.
30. **Lenardon, M. D., R. K. Whitton, C. A. Munro, D. Marshall, and N. A. R. Gow.** 2007. Individual chitin synthase enzymes synthesize microfibrils of differing structure at specific locations in the *Candida albicans* cell wall. Mol. Microbiol. **66:**1164–1173.
31. **Lipp, P., D. Thomas, M. J. Berridge, and M. D. Bootman.** 1997. Nuclear calcium signalling by individual cytoplasmic calcium puffs. EMBO J. **16:**7166–7173.
32. **Locke, E. G., M. Bonilla, L. Liang, Y. Takita, and K. W. Cunningham.** 2000. A homolog of voltage-gated Ca^{2+} channels stimulated by depletion of secretory Ca^{2+} in yeast. Mol. Cell. Biol. **20:**6686–6694.

33. **Lockhart, S. R., et al.** 2002. In *Candida albicans*, white-opaque switchers are homozygous for mating type. Genetics **162:**737–745.
34. **Lockhart, S. R., R. Zhao, K. J. Daniels, and D. R. Soll.** 2003. Alpha-pheromone-induced "shmooing" and gene regulation require white-opaque switching during *Candida albicans* mating. Eukaryot. Cell **2:**847–855.
35. **Magee, B. B., and P. T. Magee.** 2000. Induction of mating in *Candida albicans* by construction of MTLa and MTLalpha strains. Science **289:**310–313.
36. **Miller, M. G., and A. D. Johnson.** 2002. White-opaque switching in *Candida albicans* is controlled by mating-type locus homeodomain proteins and allows efficient mating. Cell **110:**293–302.
37. **Muller, E. M., E. G. Locke, and K. W. Cunningham.** 2001. Differential regulation of two Ca^{2+} influx systems by pheromone signaling in *Saccharomyces cerevisiae*. Genetics **159:**1527–1538.
38. **Muller, E. M., N. A. Mackin, S. E. Erdman, and K. W. Cunningham.** 2003. Fig1p facilitates Ca^{2+} influx and cell fusion during mating of *Saccharomyces cerevisiae*. J. Biol. Chem. **278:**38461–38469.
39. **Munro, C. A., et al.** 2007. The *PKC*, *HOG* and Ca^{2+} signalling pathways co-ordinately regulate chitin synthesis in *Candida albicans*. Mol. Microbiol. **63:**1399–1413.
40. **Peiter, E., M. Fischer, K. Sidaway, S. K. Roberts, and D. Sanders.** 2005. The *Saccharomyces cerevisiae* Ca^{2+} channel Cch1pMid1p is essential for tolerance to cold stress and iron toxicity. FEBS Lett. **579:**5697–5703.
41. **Proszynski, T. J., R. Klemm, M. Bagnat, K. Gaus, and K. Simons.** 2006. Plasma membrane polarization during mating in yeast cells. J. Cell Biol. **173:**861–866.
42. **Rispail, N., et al.** 2009. Comparative genomics of MAP kinase and calcium-calcineurin signalling components in plant and human pathogenic fungi. Fungal Genet. Biol. **46:**287–298.
43. **Shibasaki, F., E. R. Price, D. Milan, and F. McKeon.** 1996. Role of kinases and the phosphatase calcineurin in the nuclear shuttling of transcription factor NF-AT4. Nature **382:**370–373.
44. **Taylor, V., A. A. Welcher, EST Program Amgen, and U. Suter.** 1995. Epithelial membrane protein-1, peripheral myelin protein 22, and lens membrane protein 20 define a novel gene family. J. Biol. Chem. **270:**22824–22833.
45. **Van Itallie, C. M., and J. M. Anderson.** 2006. Claudins and epithelial paracellular transport. Annu. Rev. Physiol. **68:**403–429.
46. **Veses, V., and N. A. Gow.** 2008. Vacuolar dynamics during the morphogenetic transition in *Candida albicans*. FEMS Yeast Res. **8:**1339–1348.
47. **Veses, V., et al.** 2005. ABG1, a novel and essential *Candida albicans* gene encoding a vacuolar protein involved in cytokinesis and hyphal branching. Eukaryot. Cell **4:**1088–1101.
48. **Viladevall, L., et al.** 2004. Characterization of the calcium-mediated response to alkaline stress in *Saccharomyces cerevisiae*. J. Biol. Chem. **279:** 43614–43624.
49. **Wadehra, M., H. Su, L. K. Gordon, L. Goodglick, and J. Braun.** 2003. The tetraspan protein EMP2 increases surface expression of class I major histocompatibility complex proteins and susceptibility to CTL-mediated cell death. Clin. Immunol. **107:**129–136.
50. **Wu, V. M., J. Schulte, A. Hirschi, U. Tepass, and G. J. Beitel.** 2004. Sinuous is a *Drosophila* claudin required for septate junction organization and epithelial tube size control. J. Cell Biol. **164:**313–323.
51. **Wu, W., C. Pujol, S. R. Lockhart, and D. R. Soll.** 2005. Chromosome loss followed by duplication is the major mechanism of spontaneous mating-type locus homozygosis in *Candida albicans*. Genetics **169:**1311–1327.
52. **Wu, W., S. R. Lockhart, C. Pujol, T. Srikantha, and D. R. Soll.** 2007. Heterozygosity of genes on the sex chromosome regulates *Candida albicans* virulence. Mol. Microbiol. **64:**1587–1604.
53. **Yoshimura, H., T. Tada, and H. Iida.** 2004. Subcellular localization and oligomeric structure of the yeast putative stretch-activated Ca^{2+} channel component Mid1. Exp. Cell Res. **293:**185–195.
54. **Zhang, N. N., et al.** 2006. Multiple signaling pathways regulate yeast cell death during the response to mating pheromones. Mol. Biol. Cell **17:**3409–3422.
55. **Zhao, R., et al.** 2005. Unique aspects of gene expression during *Candida albicans* mating and possible G1 dependency. Eukaryot. Cell **4:**1175–1190.